



Modeling the deep penetration of outer belt electrons during the “Halloween” magnetic storm in 2003

Xinlin Li,^{1,2} A. B. Barker,^{1,3} D. N. Baker,¹ W. C. Tu,¹ T. E. Sarris,¹ R. S. Selesnick,⁴ R. Friedel,⁵ and C. Shen⁶

Received 10 June 2008; accepted 29 December 2008; published 26 February 2009.

[1] Radiation belt electrons are a natural hazard to satellites and humans in space, and they can be quickly enhanced and redistributed in the magnetosphere. Specification and advanced warning of such a reconfiguration of the electron distribution will be valuable to spacecraft designers, operators, and astronauts. Here we report our modeling results and discuss a feasible forecast procedure on such an extreme event. During the geomagnetic storm of October/November 2003, the intensity peak of the outer radiation belt electron moved from its nominal position of $L \approx 4$ to $L \approx 2.5$ in a day. This event was correlated with extremely high solar wind speeds and enhanced ULF wave power through out the inner magnetosphere, both are known to be associated with enhanced radial transport of radiation belt electrons. A radial diffusion model is developed, using the measurements of relativistic electrons at geosynchronous orbit as the source population and making the radial diffusion coefficient a function of solar wind parameters and L . We found that the deep penetration of 4.5 MeV electrons down to $L \approx 2.5$ measured by Polar High Energy Space Telescope can be modeled by the fast inward radial transport mechanism. The practical significance of this model is that the inputs are solely from measurements of current solar wind and energetic electrons at geosynchronous orbit. Thus the model can be operated in real time to forecast the multiple MeV electron fluxes inside geosynchronous orbit and down to $L \approx 2.5$ in such an extreme storm event.

Citation: Li, X., A. B. Barker, D. N. Baker, W. C. Tu, T. E. Sarris, R. S. Selesnick, R. Friedel, and C. Shen (2009), Modeling the deep penetration of outer belt electrons during the “Halloween” magnetic storm in 2003, *Space Weather*, 7, S02004, doi:10.1029/2008SW000418.

1. Introduction

[2] Electrons with energies of the order of an MeV (million electron volts), also known as “killer electrons,” can harm satellites through deep dielectric charging [e.g., *Fennell et al.*, 2001] and have a serious damaging effect on the human bodies. The Earth’s outer radiation belt consists of such relativistic electrons and normally they peak around $L \approx 4$ and decrease rapidly as L gets less than 3, where L corresponds to the radial distance in units of R_E at the equator if Earth’s magnetic field is approximated as a dipole. However, the outer radiation belt can be quickly distorted and redistributed if severe solar wind conditions occur [*Baker et al.*, 2004]. Thus, specification and forecast of

such extreme reconfiguration will be valuable to spacecraft designers and operators as well as astronauts.

[3] In this paper, we focus on a drastic variation of the outer radiation belt during the end of October and early November of 2003 known by scientists as the “Halloween storm” of 2003. The outer radiation belt was severely distorted and its center was repositioned to $L \approx 2.5$, which is rarely observed [*Baker et al.*, 2004]. We will present our modeling results of the deep penetration of these MeV electrons during this event and discuss the acceleration mechanisms and how we plan to forecast such electron variations.

[4] Several attempts have been made to understand the physical mechanisms responsible for the observed electron variations. *Horne et al.* [2005] and *Shprits et al.* [2006] suggested that the VLF (a few kilohertz) chorus acceleration mechanism would be responsible for the enhancement of ~ 2 MeV electrons at $L \approx 2.5$. They ruled out radial diffusion as a possible mechanism. *Horne et al.* [2005] argued that the intensity of ULF (2–10 millihertz) wave, which are needed for radial diffusion, decreased when the electron enhancement continued beyond 31 October.

¹Laboratory for Atmospheric and Space Physics, University of Colorado, Boulder, Colorado, USA.

²Also at Laboratory for Space Weather, Chinese Academy of Sciences, Beijing, China.

³Deceased 28 May 2005.

⁴Aerospace Corporation, Los Angeles, California, USA.

⁵Los Alamos National Laboratory, Los Alamos, New Mexico, USA.

⁶Key Laboratory for Space Weather, Chinese Academy of Sciences, Beijing, China.

Shprits et al. [2006] had the same argument and also modeled the radial diffusion process but using a constant outer boundary condition and a loss rate independent of L . They also pointed out the fact that the plasmopause was severely eroded to below $L \approx 2.5$ [Baker et al., 2004], which is a favorable condition for VLF chorus acceleration there (since the ratio of the electron plasma frequency to its cyclotron frequency is minimum just outside the plasmopause) [Summers et al., 1998; Miyoshi et al., 2003; O'Brien et al., 2003; Li et al., 2006]. Loto'aniu et al. [2006], however, from ground-based observation of ULF waves and their calculation of radial diffusion timescales, showed that the observed enhancement of ~ 2 MeV electron fluxes at $L \approx 2.5$ on 29 October is consistent with the inward radial diffusion because of drift resonance with the ULF waves but they did not model the electron fluxes to compare with observations directly. Strongly enhanced ULF waves in the inner magnetosphere on late 31 October were clearly observed by the spacecraft CLUSTER during its perigee pass [Zong et al., 2007]. Enhanced ULF waves are required in order to have fast inward radial diffusion of the electrons in addition to having a positive radial gradient of the electron's phase space density.

[5] To put the "Halloween" storm event into context, we need to remind the readers of the 24 March 1991 event, where a sudden 4 orders of magnitude enhancement of ~ 15 MeV electron fluxes with equatorial pitch angle peaked at 90° near $L = 2.5$ within tens of seconds was well measured in situ by the CRRES satellite, which was in a geotransfer orbit [Blake et al., 1992]. The CRRES event was understood as a preexisting population of ~ 1 – 2 MeV electrons at $L \approx 8$ being brought into $L = 2.5$ and accelerated in less than one drift period (150 s) of the 15 MeV electrons by a mainly inductive electric field resulting from the shock compression of the magnetosphere [Li et al., 1993].

[6] Days after the Halloween storm, 10–20 MeV electrons were observed at below $L \approx 2.5$ [Looper et al., 2005]. Kress et al. [2007] traced 1–7 MeV electrons in the outer zone in time-dependent fields from a MHD magnetospheric model simulation of the 29 October 2003 storm driven by solar wind measurements and found a newly formed 10–20 MeV electron belt near $L \approx 3$ and these 10–20 MeV electrons have a strongly peaked at 90° pitch angle distribution in the equatorial plane. Their simulation results were compared with SAMPEX measurements and seemed to be consistent with the observed delay in appearance of the peak fluxes at SAMPEX [Cook et al., 1993]. Without the in situ measurements of 10–20 MeV near the equator, it is not clear if these 10–20 MeV electrons were injected to $L \approx 2.5$ in a similar way as for the 24 March 1991 event (and were gradually pitch angle scattered into low altitude to be observable by SAMPEX), or they were produced by less dramatic inward radial diffusion, which would transport lower-energy electrons faster, or a combination of both, i.e., the shock induced electric field may transport the electrons to a lower L promptly and inward radial diffusion may transport these

electrons further inward. Because the electron fluxes rapidly decrease as the energy increases [e.g., Baker et al., 1998a], there are much more a few MeV electrons than 10–20 MeV electrons.

[7] Here we report our modeling results of electron phase space density variations before, during, and after the Halloween storm and the comparison of the model result with observation of 4.5 MeV electron fluxes at $L \approx 2.5$ measured by Polar High Energy Space Telescope (Polar/HIST) [Blake et al., 1995] during its perigee passes and discuss a feasible forecast procedure for the MeV electrons during such extreme events.

2. Observations

[8] Figure 1 shows selected solar wind parameters measured by SWEPAM and MAG instruments [McComas et al., 1998; Smith et al., 1998] on spacecraft ACE at L1 point ($\sim 240 R_E$ upstream), relativistic electron fluxes measured at geosynchronous orbit, 4.5 MeV electron flux measured by Polar at $L = 2.5$, and measured and modeled *Dst* index.

[9] All solar wind data are first averaged to ten minute intervals at ACE's position and then ballistically propagated to the Earth using the solar wind velocity. The ACE/SWEPAM instrument was not designed for solar wind speed over 1200 km/s. The solar wind speed and density data shown here were recalibrated afterward and provided by ACE/SWEPAM team, and cannot be viewed as accurate as the nominal science level 2 data (R. Skoug, private communication, 2005). A comparison between measured and modeled *Dst* index [Temerin and Li, 2006], in Figure 1, indicates that the solar wind data are rather accurate. Because the comparison is an out of sample comparison from a *Dst* model (developed on the basis of data prior to 2003) using solar wind as the only input, the model achieves a prediction efficiency of 0.914 and a linear correlation of 0.956 comparing with the measured *Dst* for an 8-year period, 1995–2002 [Temerin and Li, 2006]. The solar wind data shown in Figure 1 will be used as input to our radial diffusion model. This shows that we can also make our model operate in real time.

[10] Relativistic electron data at geosynchronous orbit are hourly averaged and combined from six Los Alamos National Laboratory (LANL) sensors on six geosynchronous satellites, widely spread in local time. These sensors are identically designed and record electron fluxes in the corresponding energy ranges. Though relativistic electron fluxes at geosynchronous orbit are a function of local time and geomagnetic activity, the LANL data shown in Figure 1 provide a good average of the relativistic electron fluxes and will be used as the source population at the outer boundary in our radial diffusion model. The average L of geosynchronous orbit is around $L = 6$ [Chen et al., 2006].

[11] The 4.5 MeV electron flux in Figure 1 is measured from Polar/HIST, which provides electron data with high resolution in energy and pitch angle [Blake et al., 1995]. However, the lower-energy channels (< 3.1 MeV) are subject to saturation when the electron fluxes are high, such

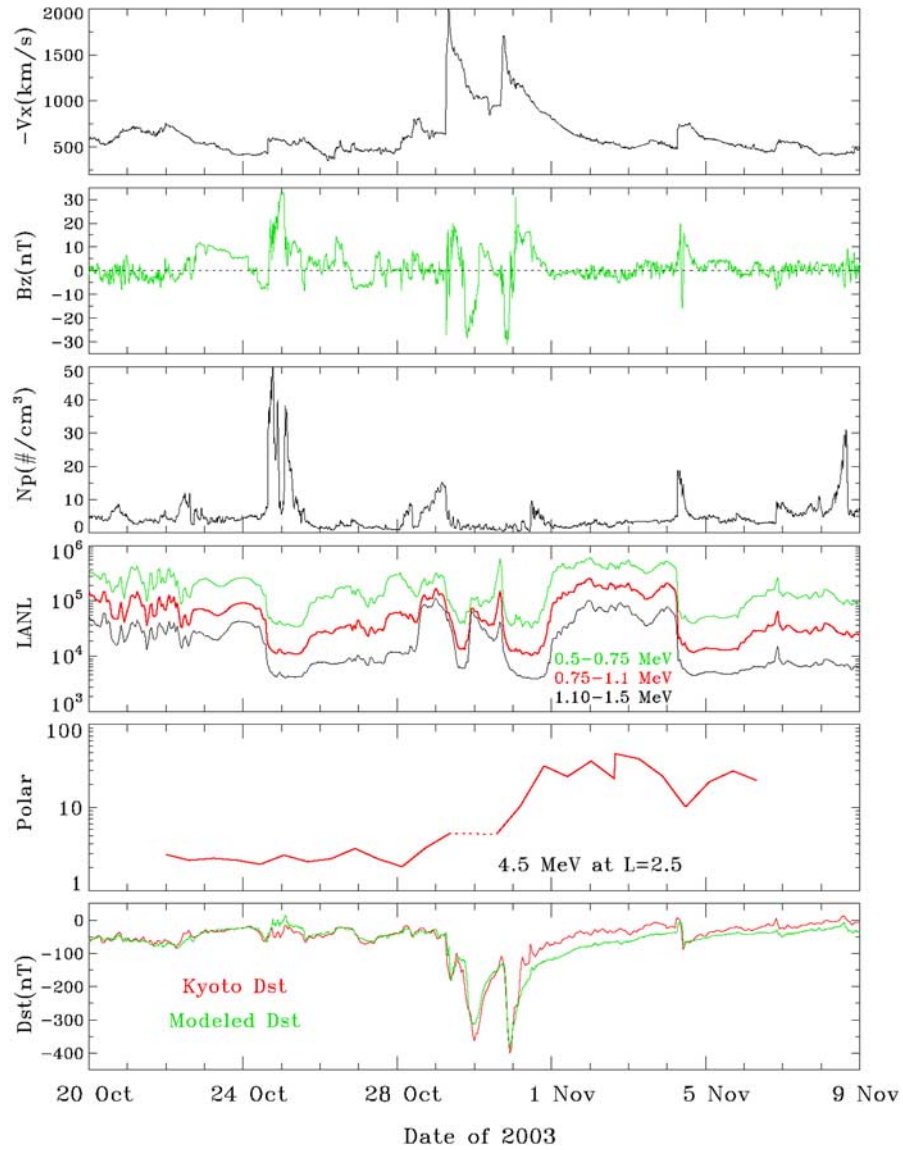


Figure 1. Selected solar wind parameters (every 10 min), hourly averaged differential electron fluxes (cm s sr MeV) combined from LANL sensors on six geosynchronous orbit satellites, differential electron fluxes measured by Polar/HIST when crossed $L = 2.5 \pm 0.2$ (note there are some data gaps, including the period covered dotted line), and measured and modeled Dst index.

as during the Halloween storm. We choose to compare our model results with the measured electrons at 4.5 MeV at $L \approx 2.5$, which are not affected by the saturation. There are factor ~ 2 uncertainties in these data because of the rapid passage of Polar through $L = 2.5$ and the averaging thereby necessitated.

3. Model

[12] Our model uses the standard radial diffusion equation [Schulz and Lanzerotti, 1974]

$$\partial f / \partial t = \{L^2 [\partial / \partial L] \{ (D_{LL} / L^2) (\partial f / \partial L) \} - f / \tau, \quad (1)$$

where f is the electron phase space density. It is related to the differential flux j by

$$f = j / p^2, \quad (2)$$

where p is the momentum of the electron. D_{LL} and τ are the diffusion coefficient and average life time of the electrons, and both are functions of L . The explicit L dependence of D_{LL} is set as

$$D_{LL} = D_0 [c_1 (L/6)^6 + (1 - c_1) (L/6)^4], \quad (3)$$

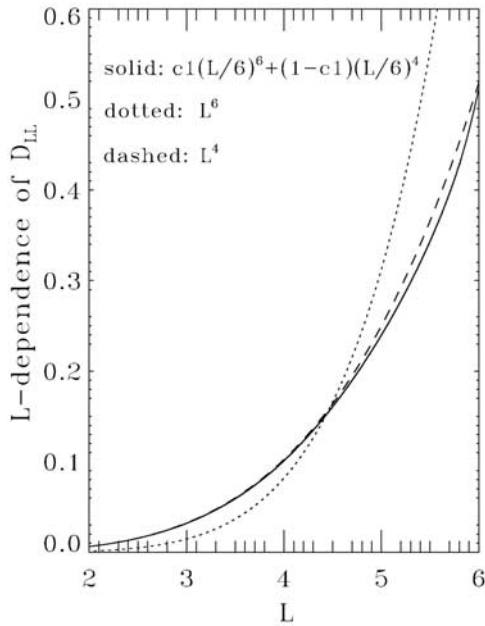


Figure 2. A comparison of L dependence of the diffusion coefficient used in the model with L^4 and L^6 .

where $c_1 = 0$ if $L < 4$ and c_1 slowly increases to 1 at $L = 6$. The rationale for such a choice of L dependence is given in next section. This L dependence is illustrated in Figure 2. The temporal part of the D_{LL} is

$$D_0 = C(v/v_0)^{\gamma_1} [1 + (v_x b_z + |v_x b_z|) \alpha^2]^{\gamma_2}, \quad (4)$$

where C is a constant that adjusts the diffusion rate, v is solar wind speed and v_0 is its average for the years 1995–1996, α is an adjustable parameter. The γ parameters determine the contribution of the two terms, which represent different ways energy can be transferred into the magnetosphere. The first term is a function of solar wind speed, whose energy can be transferred directly from dayside compression and/or through the Kelvin-Helmholtz instability from flanks [Kivelson and Russell, 1995]. The second term is a function of the convection electric field produced by the x component of the solar wind speed, v_x , and the z component of the magnetic field, b_z ; this term will be unity for northward interplanetary magnetic field (IMF), and represents the transfer because of dayside reconnection. In this paper, we present results with $C = 0.0121439/\text{day}$, $v_0 = 425 \text{ km/s}$, $\alpha = 767.614 \text{ km} \cdot \text{nT/s}$, $\gamma_1 = 2.5$, $\gamma_2 = 0.06$. These parameters were chosen, after many test runs, to give the best model results in comparison with the measurements (see Figure 5). Figure 3 shows the diffusion coefficient used in this model in comparison with others. It is clear that the diffusion coefficient we use here is significantly smaller ($L = 4-6$) and greater ($L = 2.5-3$) than the Kp -dependent diffusion coefficient used by Brautigam and Albert [2000]. This is mainly

due to the different L dependence we used (see more detailed discussion in next section).

[13] The averaged lifetime is given by $\tau = \tau_0(6/L)$, $\tau_0 = 1$ day, corresponding to the averaged lifetime of 1 day at $L = 6$ and 2.4 days at $L = 2.5$, which is consistent with recent analysis results [Thorne *et al.*, 2005].

[14] If we consider equatorial mirroring particles in a dipole field, the electron's kinetic energy and L for conserving the first adiabatic invariant, μ , will have the following relation:

$$L^3(\gamma^2 - 1) = L_0^3(\gamma_0^2 - 1), \quad (5)$$

where $\gamma = (K + 0.511)/0.511$ is the relativistic factor and K is the electron's kinetic energy in MeV. A 4.5 MeV electron at $L = 2.5$ corresponds to a 0.9 MeV at $L = 6$. On the basis of the LANL measurements shown in Figure 1, prior to 29 October, the energy spectrum can be well fitted by a power law with an index of -4 . Thus the 0.9 MeV electron flux at $L = 6$ is interpolated from the measurements from various energy channels below and above 0.9 MeV. The L in our model is the dipole L , which is equivalent to the L^* [Roderer, 1970] in a dipole magnetic field. The inner and outer boundary are set at $L = 1$ and $L = 6$, respectively. Equation (1) is solved by setting f equal to measurements of relativistic electrons at geosynchronous orbit, as the source population at the outer boundary, and D_0 as a function of solar wind parameters.

[15] We also included a decoupled process, the Dst effect to adjust f . The Dst effect is a measure of the adiabatic response of electrons to magnetic field changes [Li *et al.*, 1997b; Kim and Chan, 1997]. We implement this effect in an ad hoc way by adjusting f at all points,

$$f = f^* \exp\{[Dst(t + \Delta t) - Dst(t)]/Dst_n\}, \quad (6)$$

where Dst_n ($= 102$) determines the magnitude of the correction. If the data were given at constant values of the three adiabatic invariants, then according to Liouville's theorem, phase space density would be conserved and the above correction would be unnecessary. Since the LANL data are taken at a constant energy and radial distance instead, electrons from different μ and L values are measured (the dayside magnetosphere is compressed and the nightside is stretched).

[16] The LANL data are assigned an averaged L ($= 6$) and averaged μ . When Dst goes down (more negative), the LANL measured electron fluxes will go down. The same effect exists for the Polar/HIST measurements as well (though the effect will be smaller since we only used the measurements at low L) since the L value from Polar is from a dipole field model. The usual way to deal with this issue is to use a magnetic field model to calculate the L corresponding to the spacecraft position. However, no accurate magnetic field model exists for such an extreme event. Here we opted to use the Dst correction, equation (6), a trial and error methods, to mitigate the Dst effect,

Comparison of radial diffusion coefficients

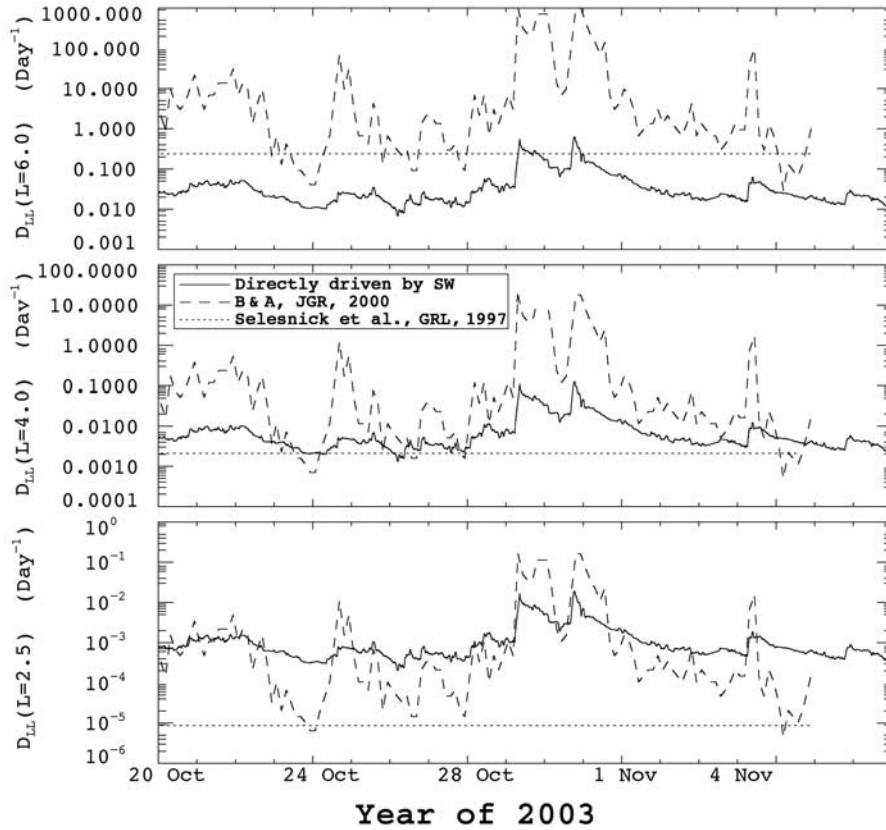


Figure 3. A comparison of the diffusion coefficient used in the model with two other published diffusion coefficients [Brautigam and Albert, 2000; Selesnick et al., 1997] at selected L .

making the modeled PSD go down as well when the Dst goes down, before directly comparing with the measurements. The parameter $Dstn$ was determined from a trial and error method to compare well the modeled results with the measurements at $L = 2.5$.

4. Results and Discussion

[17] Figure 4 shows modeled phase space density, f , of the electron with μ of 1225.5 MeV/Gauss, which is color coded, sorted by L , and plotted versus time. The f at the outer boundary, $L = 6$, is directly converted from the differential flux of electrons at 0.9 MeV measured from LANL sensors. The f at inner boundary, $L = 1$, was initially given a small value (0.0003), which has no consequence at large L . It is evident that the electrons are diffused inward, maintaining a positive radial gradient (a requirement of inward diffusion) for most of the time. Occasionally, a negative radial gradient may appear, such as around 5–6 November between $L = 4–6$, which is due to faster loss at larger L and slower inward diffusion at smaller L . At different L the f corresponds to different energy and it has

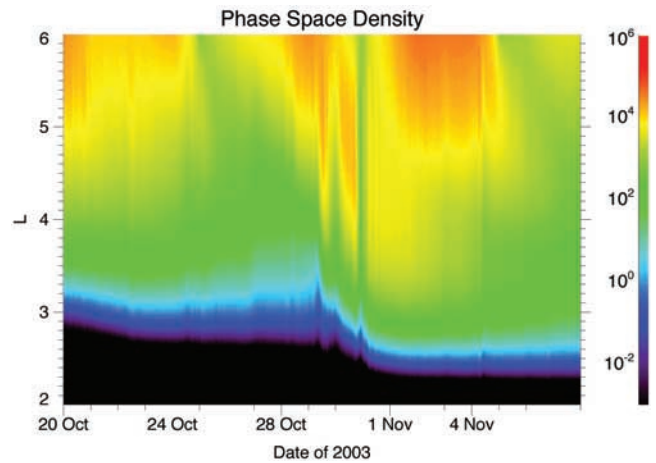


Figure 4. Modeled phase space density, f , of the electron for $\mu = 1225.5$ MeV/G (corresponding to 0.9 MeV at $L = 6$ and 4.5 MeV at $L = 2.5$). The magnitude of f is color coded, the color bar has a unit of $[10^{-10}(c/cm MeV)^3]$, and c is the speed of light.

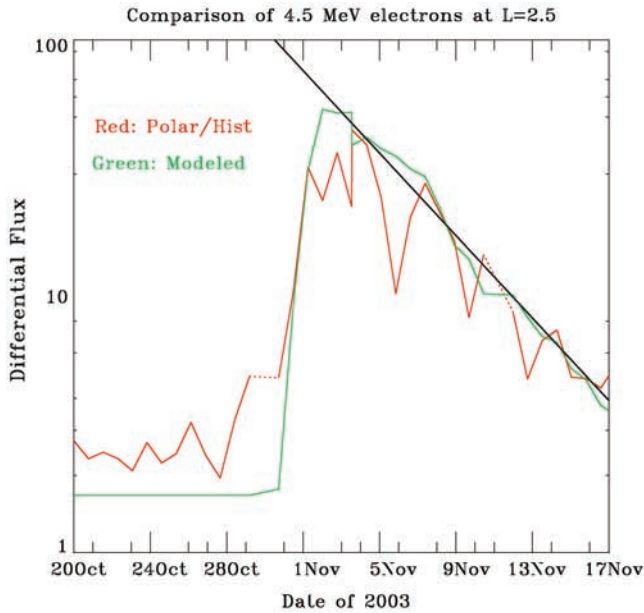


Figure 5. A comparison of measured and modeled electron fluxes at $L = 2.5$ and a fit of the decay of the electron flux with an e -folding time of 5.4 days (black line, see text for detailed discussion).

to be converted back to differential flux in order to compare with measurements.

[18] Before the Halloween storm, few MeV electrons were seen inside $L = 3$, because the diffusion coefficient is small, as shown in Figure 3. When the solar wind speed enhanced, so did the diffusion coefficient, MeV electrons showed up at and below $L = 2.5$.

4.1. Average Lifetime of the Electrons

[19] After the f at $L = 2.5$ is converted to differential flux, we can compare with the measurement, as shown in Figure 5. The modeled results more or less reproduce the measurements, the enhancement and the decay. The black line is a fit of the decay of the electron flux to an exponential with an e -folding time of 5.4 days. Baker *et al.* [2007] found that the e -folding time of 2–6 MeV for half dozen distinct acceleration (or enhancement) events seen during late 2003–2005 at $L = 2$ ranging from 8 to 35 days, which is consistent with what we found here (the e -folding time is longer at large L and for higher energy). However, we would like to emphasize that such a fit (or the e -folding time) will not give rise to the correct average lifetime because the measured electron fluxes are the net result of a balance between energization, transport, and loss [Selesnick, 2006]. When the measured electron fluxes decrease, it does not mean no more energization. It only means that the loss is more significant than energization. In the model, the actual lifetime of the electrons at $L = 2.5$ is 2.4 days, less than half of the e -folding time.

4.2. Average L Value at Geosynchronous Orbit

[20] It should be pointed out that the L values around geosynchronous orbit have large variations during magnetic storms [Chen *et al.*, 2006]. Although we have implied that the L value cannot be very accurately determined during such an extreme case, it will be still interesting to see how the L value calculated using recent empirical magnetic field models at geosynchronous orbit would actually vary during the 2003 Halloween storm period. It is known that for a given radial distance, the L value has a strong dependence on magnetic local time (MLT), we chose four fixed MLT locations for the L^* calculation, noon, midnight, dawn, and dusk, which are all on the $X - Y$ plane in GSM coordinates, with a geocentric distance of $6.6 R_E$. The results for the L^* value variations during the main part of the 2003 Halloween storm (from 28 October to 4 November) are shown in Figure 6. The L^* value is calculated every 1 h for electrons mirroring at the fixed location (local pitch angle = 90°). We used the International Geomagnetic Reference Field model as the internal magnetic field model and Tsyganenko 2001 storm model (T01S [Tsyganenko, 2002a, 2002b]) as the external field model. The models are included in the free software package, ONERA-DESP LIBRARY (D. Boscher *et al.*, ONERA-DESP LIBRARY V4.2, Toulouse-France, 2004–2008) and the inputs for the T01S model are: Dst index, solar wind speed, density, and dynamic pressure, IMF b_y and b_z in GSM coordinates. The gaps in the L^* plots indicate the time when the drift shell is open and L^* is not defined (the drift path is not closed), on the basis of the empirical magnetic model.

[21] It is evident that the electrons at geosynchronous orbit can often be on open drift paths, depending on the MLT and also the geomagnetic conditions. Electrons started on open drift paths can be transported into close ones and vice versa. The measurements shown in Figure 1 are averaged from six LANL satellites, widely spread in local time, which would give a good approximation of electron populations around $L^* = 6$ during less active times. The caveat demonstrated by Figure 6 is that the L^* value varies largely and sometimes drift shell is not even closed during strong storm times.

4.3. Open Question of the Origin of MeV Electrons in the Magnetosphere

[22] It should also be pointed out that it is still an open question as to how the 0.9 MeV electrons at geosynchronous orbit, the source population used in this model, are energized [Selesnick and Blake, 2000], though from direct comparison between the solar wind energetic electrons and energetic electrons at geosynchronous orbit show that they have to be energized inside the magnetosphere (not directly diffusing in from the solar wind) [Li *et al.*, 1997a].

4.4. L dependence of the Diffusion Coefficient

[23] Another open question is about the L dependence of the diffusion coefficient. As shown in Figure 3, the

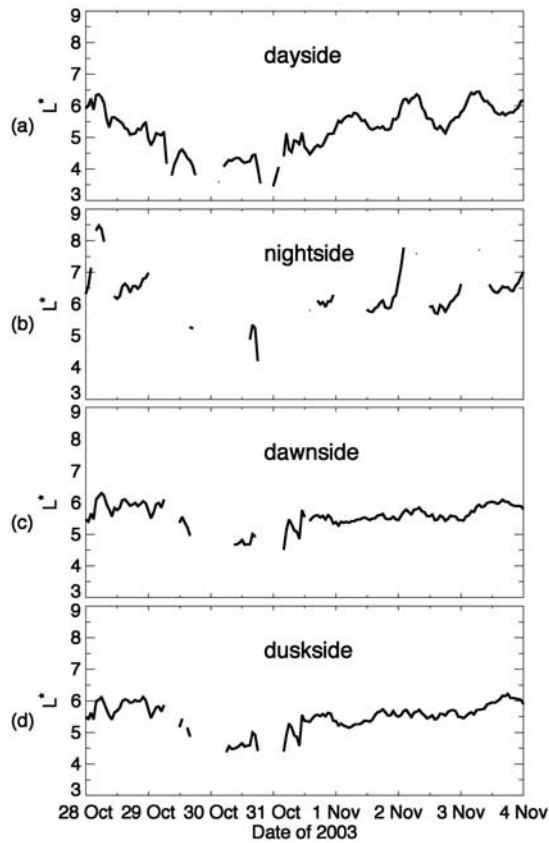


Figure 6. L^* values at geosynchronous orbit during the 2003 Halloween storm. The L^* values are calculated for electrons located at four different MLTs on the $X - Y$ plane in GSM coordinates, with geocentric distance of $6.6 R_E$. The electrons have 90° local pitch angle at the given position. The L^* is calculated every 1 h using the International Geomagnetic Reference Field model as the internal magnetic field model and the Tsyganenko 2001 storm model as the external magnetic field model. The gaps mean that L^* is not defined (the electrons are open drift paths).

magnitude of the diffusion coefficient in our model is not particularly large, but its L dependence is very different from the commonly assumed L^{10} [Brautigam and Albert, 2000], thus the diffusion here is less significant at greater L but more significant at lower L . Shprits *et al.* [2006] used Brautigam and Albert's [2000] diffusion coefficient (applicable for Kp up to 6) and a constant outer boundary conditions at $L = 7$. From Figure 1, it is clear that the electron fluxes at geosynchronous orbit are not constant. From Figure 3, it is evident that Brautigam and Albert's [2000] diffusion coefficient is smaller than our diffusion coefficient at $L = 2.5$ for most of the time, except for the time period with $Kp > 6$. Shprits *et al.* [2006] also used a shorter life time, $\tau = 3/Kp$, during active periods. Thus it is understandable why Shprits *et al.* [2006] believed that

radial diffusions could not account for the observed electron enhancements. The actual L dependence of the diffusion coefficient at different L region is still an unresolved problem [Fei *et al.*, 2006; Sarris *et al.*, 2006] mainly because the actual power of the ULF waves as a function of L is not certain. Statistically, the ULF wave power is proportional to the L values on the basis of ground magnetic field measurements and is also proportional to the solar wind speed [Mathie and Mann, 2001]. However, during active times, electric field can penetrate deep into inner magnetosphere, stronger at lower- L region [Rowland and Wygant, 1998]. Applying global MHD simulations to this particular event, Kress *et al.* [2007] showed that the magnitude of the electric field could be tens of mV/m or greater during the sudden storm commencement. This kind of electric field can transport (because of EB drift) charged particles very quickly.

[24] The diffusion coefficients determined from magnetic field measurements at $L = 4$ [Lanzerotti and Morgan, 1973] and $L = 6.6$ [Lanzerotti *et al.*, 1978] showed different scalings with L for different Kp . For $Kp = 1$ the diffusion coefficient goes as L^{19} while for $Kp = 6$ it goes as L^6 [Perry *et al.*, 2005]. During the Halloween storm, Kp is greater than 6. The power of 4–6 on L used in this paper seems reasonable. While the exact L dependence should be further investigated and debated, our model shows that electrons can be radially diffused into $L = 2.5$ if the solar wind speed is high enough. There have been numerous studies showing the strong correlations between solar wind speed and the ULF wave power [Engebretson *et al.*, 1998; Vennerstrom, 1999] and between the enhanced ULF wave power and the enhanced radiation belt electrons [Rostoker *et al.*, 1998; Hudson *et al.*, 1999; Baker *et al.*, 1998b; Mathie and Mann, 2001; Loto'aniu *et al.*, 2006; Zong *et al.*, 2007]. In addition, recent statistical study of the outer belt associated with coronal hole streams by Miyoshi and Kataoka [2008] showed that not only solar wind speed but also small amplitude of the southward IMF b_z within coronal hole stream is essential for the large flux enhancement of the outer belt.

4.5. Inward Radial Transport Versus In Situ Heating

[25] It has been a long-standing question of the physical processes responsible for the outer belt variations in general [e.g., Li and Temerin, 2001; Friedel *et al.*, 2002; Reeves *et al.*, 2003; Miyoshi *et al.*, 2004; Tu *et al.*, 2008]. It is not expected that there will be a quick resolve on this question.

[26] Recently the paradigm for explaining the creation of the electron radiation belt has been shifting from one using almost exclusively the theory of radial diffusion to one emphasizing more the role of waves [Horne *et al.*, 2005; Shprits *et al.*, 2006; Chen *et al.*, 2007; Bortnik and Thorne, 2007; Albert, 2008], presumably chorus whistler waves, in the heating of radiation belt electrons. However, it is difficult to distinguish the two acceleration mechanisms [Degeling *et al.*, 2008].

[27] For the case presented in this paper, radial diffusion makes a connection between the boundary conditions at $L = 6$ and the phase space density at $L = 2.5$, reproducing the measurements at $L = 2.5$. But there is another way to make this connection other than radial diffusion at constant first and second adiabatic invariant. We know that low- and high-energy electrons at $L = 6$ are well correlated, with high-energy electrons delayed with respect to the low energy [Li *et al.*, 2005; Turner and Li, 2008]. We also know that low-energy electrons can be transported to lower L fast, either by direct convection or fast radial diffusion, and that such electrons can act as source for further heating, which produces high-energy electrons locally. Such a scenario could have been mimicked by radial diffusion.

4.6. Real Time Forecast of MeV Electrons

[28] While the detailed physical processes relating the solar wind and MeV electrons are still being investigated, efforts have been made to predict and forecast these relativistic electrons at geosynchronous orbit on the basis of solar wind measurements [Baker *et al.*, 1990; Li *et al.*, 2001; Li, 2004; Barker *et al.*, 2005]. In fact we are now forecasting >2 MeV electrons at geosynchronous orbit 1 to 2 days in advance using real time solar wind data from ACE. This forecast model has been running in real time and the results are updated every hour on the Website: lasp.colorado.edu/~lix (click Real Time Forecast . . .), available to the community and the public. Therefore, we can combine our current real time forecast model at geosynchronous orbit and the model described here to forecast the electron variations both at and inside geosynchronous orbit.

5. Conclusions

[29] The Earth's radiation environment is much more dynamical than any statistical models, such as AE8 model [Vette, 1991], suggest. Taking advantage of the normally benign radiation environment at $L < 3$, many spacecraft systems operate in the middle Earth orbit (MEO) altitude range. Events such as the Halloween storm can drastically change the radiation environment around the MEO and there suddenly develops a hostile space weather situation in a region that normally is quiescent. Understanding what physical processes can cause such as a sudden change and forecasting the outer radiation belt variations during such extreme events are of significant importance in science and application.

[30] We have investigated the deep penetration of MeV electrons into the inner magnetosphere during the October–November 2003 magnetic storm. We model the electron variations by a radial diffusion model, which uses the actual measurements of electron fluxes at geosynchronous orbit as the outer boundary, a realistic loss term, and a diffusion coefficient directly depending on solar wind parameters, mostly the solar wind speed. Though physical mechanism responsible for the enhancement of multiple

MeV electrons at $L = 2.5$ is still debated, our radial diffusion model results show that the enhancement of 4.5 MeV electrons at $L = 2.5$ can be attributed to inward radial transport because there is no local heating in our radial diffusion model and the only electron source is the measured electron flux at geosynchronous orbit.

[31] The daily variation of >2 MeV electrons at geosynchronous orbit has been forecast in realtime up to 48 h in advance using real time solar wind data from ACE and real time electron data from GOES satellite (<http://lasp.colorado.edu/~lix/>). We plan to include the model presented here into our operational model to forecast multiple MeV electrons inside geosynchronous orbit for such extreme events.

[32] **Acknowledgments.** This work was supported by NSF grants (Center for Integrated Space Weather Modeling ATM-0120950 and ATM-0519207) and also by grants from National Natural Science Foundation of China 40621003 and 40728005.

References

- Albert, J. M. (2008), Efficient approximations of quasi-linear diffusion coefficients in the radiation belts, *J. Geophys. Res.*, *113*, A06208, doi:10.1029/2007JA012936.
- Baker, D. N., R. L. McPherron, T. E. Cayton, and R. W. Klebesadel (1990), Linear Prediction filter analysis of relativistic electron properties at 6.6 R_E , *J. Geophys. Res.*, *95*, 15,133–15,140, doi:10.1029/JA095iA09p15133.
- Baker, D. N., X. Li, J. B. Blake, and S. Kanekal (1998a), Strong electron acceleration in the Earth's magnetosphere, *Adv. Space Res.*, *21*(4), 609–613, doi:10.1016/S0273-1177(97)00970-8.
- Baker, D. N., et al. (1998b), A strong CME-related magnetic cloud interaction with the Earth's magnetosphere: ISTP observation of rapid relativistic electron acceleration on May 15, 1997, *Geophys. Res. Lett.*, *25*, 2975–2978, doi:10.1029/98GL01134.
- Baker, D. N., S. G. Kanekal, X. Li, S. P. Monk, J. Goldstein, and J. L. Burch (2004), An extreme distortion of the Van Allen belt arising from the 'Halloween' solar storm in 2003, *Nature*, *432*, 878–881, doi:10.1038/nature03116.
- Baker, D. N., S. G. Kanekal, R. B. Horne, N. P. Meredith, and S. A. Glauert (2007), Low-altitude measurements of 2–6 MeV electron trapping lifetimes at $1.5 \leq L \leq 2.5$, *Geophys. Res. Lett.*, *34*, L20110, doi:10.1029/2007GL031007.
- Barker, A., X. Li, and R. S. Selesnick (2005), Modeling the radiation belt electrons with radial diffusion driven by the solar wind, *Space Weather*, *3*, S10003, doi:10.1029/2004SW000118.
- Blake, J. B., W. A. Kolasinski, R. W. Fillius, and E. G. Mullen (1992), Injection of electrons and protons with energies of tens of MeV into $L < 3$ on 24 March 1991, *Geophys. Res. Lett.*, *19*, 821–824, doi:10.1029/92GL00624.
- Blake, J. B., et al. (1995), CEPPAD: Comprehensive Energetic Particle and Pitch Angle Distribution Experiment (CEPPAD) on POLAR, *Space Sci. Rev.*, *71*, 531–562, doi:10.1007/BF00751340.
- Bortnik, J., and R. M. Thorne (2007), The dual role of ELF/VLF chorus waves in the acceleration and precipitation of radiation belt electrons, *J. Atmos. Sol. Terr. Phys.*, *69*, 378–386, doi:10.1016/j.jastp.2006.05.030.
- Brautigam, D. H., and J. M. Albert (2000), Radial diffusion analysis of outer radiation belt electrons during the 9 October 1990 magnetic storm, *J. Geophys. Res.*, *105*, 291–309, doi:10.1029/1999JA900344.
- Chen, Y., R. H. W. Friedel, and G. D. Reeves (2006), Phase space density distributions of energetic electrons in the outer radiation belt during two Geospace Environment Modeling Inner Magnetosphere/Storms selected storms, *J. Geophys. Res.*, *111*, A11S04, doi:10.1029/2006JA011703.

- Chen, Y., G. D. Reeves, and R. H. W. Friedel (2007), The energization of relativistic electrons in the outer Van Allen radiation belt, *Nat. Phys.*, *3*, 614–617, doi:10.1038/nphys655.
- Cook, W. R., et al. (1993), PET: A proton/electron telescope for studies of magnetospheric, solar, and galactic particles, *IEEE Trans. Geosci. Remote Sens.*, *31*, 565–571, doi:10.1109/36.225523.
- Degeling, A. W., L. G. Ozeke, R. Rankin, I. R. Mann, and K. Kabin (2008), Drift resonant generation of peaked relativistic electron distributions by Pc 5 ULF waves, *J. Geophys. Res.*, *113*, A02208, doi:10.1029/2007JA012411.
- Engebretson, M., K.-H. Glassmeier, M. Stellmacher, W. J. Hughes, and H. Luehr (1998), The dependence of high-latitude Pc5 wave power on solar wind velocity and on the phase of high-speed solar wind streams, *J. Geophys. Res.*, *103*, 26,271–26,283, doi:10.1029/97JA03143.
- Fei, Y., A. A. Chan, S. R. Elkington, and M. J. Wiltberger (2006), Radial diffusion and MHD particle simulations of relativistic electron transport by ULF waves in the September 1998 storm, *J. Geophys. Res.*, *111*, A12209, doi:10.1029/2005JA011211.
- Fennell, J. F., H. C. Koons, J. L. Roeder, and J. B. Blake (2001), Spacecraft charging: Observations and relationship to satellite anomalies, paper presented at 7th Spacecraft Charging Technology Conference, Eur. Space Agency, Noordwijk, Netherlands, 23–27 April.
- Friedel, R. H. W., G. Reeves, and T. Obara (2002), Relativistic electron dynamics in the inner magnetosphere - a review, *J. Atmos. Sol. Terr. Phys.*, *64*, 265–282, doi:10.1016/S1364-6826(01)00088-8.
- Horne, R. B., et al. (2005), Wave acceleration of electrons in the Van Allen radiation belts, *Nature*, *437*, 227–230, doi:10.1038/nature03939.
- Hudson, M. K., et al. (1999), Simulation of radiation belt dynamics driven by solar wind variations, in *Sun-Earth Plasma Connections*, *Geophys. Monogr. Ser.*, vol. 109, edited by J. L. Burch, R. L. Carovillano, and S. K. Antiochos, pp. 171–182, AGU, Washington, D. C.
- Kim, H.-J., and A. A. Chan (1997), Fully adiabatic changes in storm-time relativistic electron fluxes, *J. Geophys. Res.*, *102*, 22,107–22,116, doi:10.1029/97JA01814.
- Kivelson, M. G., and C. T. Russell (1995), *Pulsations and Magnetohydrodynamics Waves: Introduction to Space Physics*, Cambridge Univ. Press, Cambridge, U. K.
- Kress, B. T., M. K. Hudson, M. D. Looper, J. Albert, J. G. Lyon, and C. C. Goodrich (2007), Global MHD test particle simulations of >10 MeV radiation belt electrons during storm sudden commencement, *J. Geophys. Res.*, *112*, A09215, doi:10.1029/2006JA012218.
- Lanzerotti, L. J., and C. G. Morgan (1973), ULF geomagnetic power near $L = 4$: 2. Temporal variation of the radial diffusion coefficient for relativistic electrons, *J. Geophys. Res.*, *78*, 4600–4610, doi:10.1029/JA078i022p04600.
- Lanzerotti, L. J., D. C. Webb, and C. W. Arthur (1978), Geomagnetic field fluctuations at synchronous orbit: 2. Radial diffusion, *J. Geophys. Res.*, *83*, 3866–3870, doi:10.1029/JA083iA08p03866.
- Li, X. (2004), Variations of 0.7–6.0 MeV electrons at geosynchronous orbit as a function of solar wind, *Space Weather*, *2*(3), S03006, doi:10.1029/2003SW000017.
- Li, X., and M. Temerin (2001), The electron radiation belt, *Space Sci. Rev.*, *95*(1–2), 569–580, doi:10.1023/A:1005221108016.
- Li, X., I. Roth, M. Temerin, J. Wygant, M. K. Hudson, and J. B. Blake (1993), Simulation of the prompt energization and transport of radiation particles during the March 24, 1991 SSC, *Geophys. Res. Lett.*, *20*, 2423–2426, doi:10.1029/93GL02701.
- Li, X., D. N. Baker, M. Temerin, D. Larson, R. P. Lin, G. D. Reeves, M. Looper, S. G. Kanekal, and R. A. Mewaldt (1997a), Are energetic electrons in the solar wind the source of the outer radiation belt?, *Geophys. Res. Lett.*, *24*(8), 923–926, doi:10.1029/97GL00543.
- Li, X., D. N. Baker, M. Temerin, T. E. Cayton, G. D. Reeves, R. A. Christensen, J. B. Blake, M. D. Looper, R. Nakamura, and S. G. Kanekal (1997b), Multisatellite observations of the outer zone electron variation during the November 3–4, 1993, magnetic storm, *J. Geophys. Res.*, *102*, 14,123–14,140, doi:10.1029/97JA01101.
- Li, X., M. Temerin, D. N. Baker, G. D. Reeves, and D. Larson (2001), Quantitative prediction of radiation belt electrons at geostationary orbit based on solar wind measurements, *Geophys. Res. Lett.*, *28*, 1887–1890, doi:10.1029/2000GL012681.
- Li, X., D. N. Baker, M. Temerin, G. D. Reeves, R. Friedel, and C. Shen (2005), Energetic electrons, 50 keV to 6 MeV, at geosynchronous orbit: Their responses to solar wind variations, *Space Weather*, *3*, S04001, doi:10.1029/2004SW000105.
- Li, X., D. N. Baker, T. P. O'Brien, L. Xie, and Q. G. Zong (2006), Correlation between the inner edge of outer radiation belt electrons and the innermost plasmopause location, *Geophys. Res. Lett.*, *33*, L14107, doi:10.1029/2006GL026294.
- Looper, M. D., J. B. Blake, and R. A. Mewaldt (2005), Response of the inner radiation belt to the violent Sun-Earth connection events of October/November 2003, *Geophys. Res. Lett.*, *32*, L03S06, doi:10.1029/2004GL021502.
- Loto'aniu, T. M., I. R. Mann, L. G. Ozeke, A. A. Chan, Z. C. Dent, and D. K. Milling (2006), Radial diffusion of relativistic electrons into the radiation belt slot region during the 2003 Halloween geomagnetic storms, *J. Geophys. Res.*, *111*, A04218, doi:10.1029/2005JA011355.
- Mathie, R. A., and I. R. Mann (2001), On the solar wind control of Pc5 ULF pulsation power at midlatitudes: Implications for MeV electron acceleration in the outer radiation belt, *J. Geophys. Res.*, *106*(A12), 29,783–29,796, doi:10.1029/2001JA000002.
- McComas, D. J., et al. (1998), Solar Wind Electron Proton Alpha Monitor (SWEPAM) for the Advanced Composition Explorer, *Space Sci. Rev.*, *86*, 563–612, doi:10.1023/A:1005040232597.
- Miyoshi, Y. S., and R. Kataoka (2008), Flux enhancement of the outer radiation belt electrons after the arrival of stream interaction regions, *J. Geophys. Res.*, *113*, A03S09, doi:10.1029/2007JA012506.
- Miyoshi, Y. S., A. Morioka, T. Obara, H. Misawa, T. Nagai, and Y. Kasahara (2003), Rebuilding process of the outer radiation belt during the 3 November 1993 magnetic storm: NOAA and Exos-D observations, *J. Geophys. Res.*, *108*(A1), 1004, doi:10.1029/2001JA007542.
- Miyoshi, Y. S., V. K. Jordanova, A. Morioka, and D. S. Evans (2004), Solar cycle variations of the electron radiation belts: Observations and radial diffusion simulation, *Space Weather*, *2*, S10S02, doi:10.1029/2004SW000070.
- O'Brien, T. P., et al. (2003), Energization of relativistic electrons in the presence of ULF power and MeV microbursts: Evidence for dual ULF and VLF acceleration, *J. Geophys. Res.*, *108*(A8), 1329, doi:10.1029/2002JA009784.
- Perry, K. L., M. K. Hudson, and S. R. Elkington (2005), Incorporating spectral characteristics of Pc5 waves into three-dimensional radiation belt modeling and the diffusion of relativistic electrons, *J. Geophys. Res.*, *110*, A03215, doi:10.1029/2004JA010760.
- Reeves, G. D., K. L. McAdams, R. H. W. Friedel, and T. P. O'Brien (2003), Acceleration and loss of relativistic electrons during geomagnetic storms, *Geophys. Res. Lett.*, *30*(10), 1529, doi:10.1029/2002GL016513.
- Roderer, J. G. (1970), *Dynamics of Geomagnetically Trapped Radiation*, Springer, New York.
- Rostoker, G., S. Skone, and D. N. Baker (1998), On the origin of relativistic electrons in the magnetosphere associated with some geomagnetic storms, *Geophys. Res. Lett.*, *25*, 3701–3704, doi:10.1029/98GL02801.
- Rowland, D., and J. R. Wygant (1998), The dependence of the large scale electric field in the inner magnetosphere on magnetic activity, *J. Geophys. Res.*, *103*, 14,959–14,964, doi:10.1029/97JA03524.
- Sarris, T. E., X. Li, and M. Temerin (2006), Simulating radial diffusion of energetic (MeV) electrons through a model of fluctuating electric and magnetic fields, *Ann. Geophys.*, *24*, 1–16.
- Schulz, M., and L. Lanzerotti (1974), *Particle Diffusion in the Radiation Belts*, Springer, New York.
- Selesnick, R. S. (2006), Source and loss rate of radiation belt relativistic electrons during magnetic storms, *J. Geophys. Res.*, *111*, A04210, doi:10.1029/2005JA011473.
- Selesnick, R. S., and J. B. Blake (2000), On the source location of radiation belt relativistic electrons, *J. Geophys. Res.*, *105*, 2607–2624, doi:10.1029/1999JA900445.

- Selesnick, R. S., J. B. Blake, W. A. Kolasinski, and T. A. Fritz (1997), A quiescent state of 3 to 8 MeV radiation belt electrons, *Geophys. Res. Lett.*, *24*, 1343–1346, doi:10.1029/97GL51407.
- Shprits, Y. Y., R. M. Thorne, R. B. Horne, S. A. Glauert, M. Cartwright, C. T. Russell, D. N. Baker, and S. G. Kanekal (2006), Acceleration mechanism responsible for the formation of the new radiation belt during the 2003 Halloween solar storm, *Geophys. Res. Lett.*, *33*, L05104, doi:10.1029/2005GL024256.
- Smith, C. W., et al. (1998), The ACE magnetic field experiment, *Space Sci. Rev.*, *86*(613), doi:10.1023/A:1005092216668.
- Summers, D., R. Thorne, and F. Xiao (1998), Relativistic theory of wave-particle resonant diffusion with application to electron acceleration in the magnetosphere, *J. Geophys. Res.*, *103*(A9), 20,487–20,500, doi:10.1029/98JA01740.
- Temerin, M., and X. Li (2006), *Dst* model for 1995–2002, *J. Geophys. Res.*, *111*, A04221, doi:10.1029/2005JA011257.
- Thorne, R. M., T. P. O'Brien, Y. Y. Shpritz, D. Summers, and R. B. Horne (2005), Timescale for MeV electron microburst loss during geomagnetic storms, *J. Geophys. Res.*, *110*, A09202, doi:10.1029/2004JA010882.
- Tsyganenko, N. A. (2002a), A model of the near magnetosphere with a dawn-dusk asymmetry: 1. Mathematical structure, *J. Geophys. Res.*, *107*(A8), 1179, doi:10.1029/2001JA000219.
- Tsyganenko, N. A. (2002b), A model of the near magnetosphere with a dawn-dusk asymmetry: 2. Parameterization and fitting to observations, *J. Geophys. Res.*, *107*(A8), 1176, doi:10.1029/2001JA000220.
- Tu, W., X. Li, Y. Chen, G. D. Reeves, and M. Temerin (2008), Storm-dependent radiation belt dynamics, *J. Geophys. Res.*, doi:10.1029/2008JA013480, in press.
- Turner, D., and X. Li (2008), Quantitative forecast of relativistic electron flux at geosynchronous orbit based on low-energy electron flux, *Space Weather*, *6*, S05005, doi:10.1029/2007SW000354.
- Vennerstrom, S. (1999), Dayside magnetic ULF power at high latitudes: A possible long-term proxy for the solar wind velocity?, *J. Geophys. Res.*, *104*, 10,145–10,157, doi:10.1029/1999JA900015.
- Vette, J. (1991), The AE-8 trapped electron model environment, *Rep. NSSDC91-24*, NASA, Greenbelt, Md.
- Zong, Q. G., et al. (2007), Energetic particle modulation in the dayside magnetosphere, *Geophys. Res. Lett.*, *34*, L12105, doi:10.1029/2007GL029915.

D. N. Baker, X. Li, W. C. Tu, and T. E. Sarris, Laboratory for Atmospheric and Space Physics, University of Colorado, 1234 Innovation Drive, Boulder, CO 80303-7814, USA. (lix@lasp.colorado.edu)

R. Friedel, Los Alamos National Laboratory, 30 Bikini Atoll Road, Mail Stop D436, Los Alamos, NM 87545, USA.

R. S. Selesnick, Aerospace Corporation, P.O. Box 92957, Los Angeles, CA 90009-2957, USA.

C. Shen, Key Laboratory for Space Weather, Chinese Academy of Sciences, P. O. Box, 8701, Beijing 100080, China.